Vibrational Control of an Exothermic Reaction in a CSTR: Theory and Experiments

Vibrational control is a method for modification of dynamic properties of linear and nonlinear systems by introducing fast, zero-average oscillations in the system's parameters. In this paper, forced oscillations introduced in the input flow rates of an exothermic continuous stirred-tank reactor (CSTR) are shown to result in a modification of the *S*-shaped steady state curve. This modification leads to a possibility of operating a CSTR at an asymptotically stable period regime located in the vicinity of an unstable steady state of the reactor system with stationary input flow rates. Thus, vibrations of the input flow rates can be viewed as a stabilizing mechanism for exothermic CSTR's.

Ali Cinar, Jian Deng,
S. M. Meerkov, Xianshu Shu
Departments of Chemical Engineering
and Electrical Engineering
Illinois Institute of Technology
Chicago, IL 60616

Introduction

Vibrational control is an open-loop control method that modifies the properties of linear and nonlinear systems by introducing fast, zero-average parametric oscillations. The theory of vibrational control has been developed by Meerkov (1980, 1982) and Bellman et al. (1983b, 1984a,b), where the conditions of vibrational stabilizability and vibrational controllability have been derived using the method of averaging (Bogoliubov and Mitropolsky, 1961; Minorsky, 1962). A hypothetical application of vibrational control to chemical reactions has been discussed by Bellman et al. (1983a) and some preliminary results on asymptotically stable periodic operation of an exothermic continuous stirred-tank reactor (CSTR) in the vicinity of an unstable steady state by means of vibrational control have been reported by Cinar et al. (1984).

Operation of a CSTR near or at an unstable steady state is of considerable importance. In many situations these states offer optimal yield, given the technological constraints—for instance, the maximum admissible temperature in the reactor. Often, the operation of a reactor at an unstable steady state can be achieved by feedback control (Aris and Amundson, 1958a–c; Douglas, 1972; Ding et al., 1974; Chang and Schmitz, 1975a,b). There are, however, difficulties: the application of feedback requires on-line measurements of states that may be impossible in some cases or may involve large delays and the manipulated variables may reach their constraint boundaries. For exothermic CSTR control, if the reactor temperature is regulated by varying the properties of a coolant stream considerable energy expenses are involved.

Vibrational control offers a way to avoid these difficulties. In application to CSTR's, vibrational control is introduced through appropriately designed periodic oscillations of the input flow rates. This in turn ensures an asymptotically stable periodic operation of the reactor in the vicinity of an unstable steady state. That is the phenomenon studied in this paper using a second-order exothermic reaction between sodium thiosulfate, $Na_2S_2O_3$, and hydrogen peroxide, H_2O_2, as an example.

Besides vibrational control, there have been other approaches to periodic operation of chemical reactors (see review articles by Bailey 1973, 1977). These approaches include periodic optimization (Rinaldi, 1970; Bailey and Horn, 1971; Matsubara et al., 1974; Gilbert, 1977), push-pull control (Bruns and Bailey, 1975, 1977), and asynchronous quenching (Fjeld, 1974). The first two approaches are based on feedback strategies and therefore require measurements of the states. Asynchronous quenching is an open-loop technique and is very much akin to the vibrational control approach. It has been used to study quenching of autoperiodic oscillations (Fjeld, 1968) and to obtain new steady states that are not in the stationary steady state solution set by choosing appropriate controls that switch infinitely fast (Fjeld, 1974). However, the theory of asynchronous quenching does not seem to give the conditions under which the stabilization can be achieved. For this reason, vibrational control has been chosen in this study as a technique for periodic operation of a reactor in the vicinity of an unstable steady state.

On the basis of analytical, numerical, and experimental studies, the results reported here show that *appropriately* introduced periodic oscillations of the input flow rates indeed ensure an

Correspondence concerning this paper should be addressed to Ali Cinar.
The current address of S. M. Meerkov is Department of Electrical Engineering and Computer Science, The University of Michigan, Ann Arbor, MI 48109.

asymptotically stable periodic operation of an exothermic CSTR in the vicinity of an unstable equilibrium point. If some theoretical indications on the existence of this phenomenon have been known before (Fjeld, 1974; Bellman et al., 1983a), the present work is the *first time* that *experiments* have been carried out and that a good agreement with analytical and numerical predictions has been shown. Also for the first time, this paper gives a procedure for choosing parameters (frequencies, amplitudes, etc.) of the *appropriate* vibrations so that the stabilizing effect can be achieved. These are the main practical contributions of the paper.

A theoretical contribution of the paper is based on an asymptotic method for analysis of nonlinear systems with fast parametric oscillations. Using this method, it is shown that the average S-shaped steady state curve of a reactor with vibrations has a smaller negative slope (unstable) part compared with a reactor having stationary inputs. This explains why asymptotically stable operation of a reactor in the vicinity of an unstable steady state is possible.

The significance of the reported work can be found in the fact that vibrational control is shown to be a viable method of control for unstable chemical plants. Used by itself or along with a feedback strategy, vibrational control can be a useful and economical alternative method of control in reaction engineering.

The content of the paper is as follows. After a description of the reaction and reactor system under consideration with stationary inputs,

1. The model of the reaction-reactor system with periodic inputs is derived.
2. An asymptotic analysis of the model equations obtained is carried out.
3. A procedure for choosing the parameters of stabilizing vibrations is formulated.
4. Results of a numerical investigation of the equations obtained are reported.
5. Experiments, carried out with a reactor system having oscillating input flows, are described.

The method, used in analysis along the lines of 1–3 above, is general in nature and can be used for a large class of chemical reactors modeled by ordinary differential equations with oscillating parameters. This method is described in the Appendix.

The Reactor System

The second-order exothermic reaction between sodium thiosulfate, $Na_2S_2O_3$, and hydrogen peroxide, H_2O_2, in aqueous solution is used in conducting the vibrational control studies with a CSTR. This reaction has been used extensively in experimental and theoretical studies on multiplicity of steady states in chemical reactors (Root and Schmitz, 1969; Vetjasa and Schmitz, 1970; Schmitz et al., 1979; Ausikaitis and Engel, 1974; Lin, 1980) and on control of stirred-tank reactors (Chang and Schmitz, 1975a,b). The stoichiometric equation for the reaction is

$$2Na_2S_2O_3 + 4H_2O_2 \rightarrow Na_2S_2O_6 + Na_2SO_4 + 4H_2O.$$

A pilot plant unit has been constructed in the Chemical Enginering Department at IIT to conduct the experiments. The system consists of two feed storage tanks, a CSTR reactor, digital thermometers and two automatic control valves, Figure 1. The thermometers and the control valves are interfaced with a DEC LSI-11/23 microcomputer. The computer is used to monitor and store the temperature information and to issue control signals to the reactant control valves. The feed tanks are housed in an ice bath to reduce the reactant storage temperature; the reactants in the tanks are pressurized by compressed air. The reac-

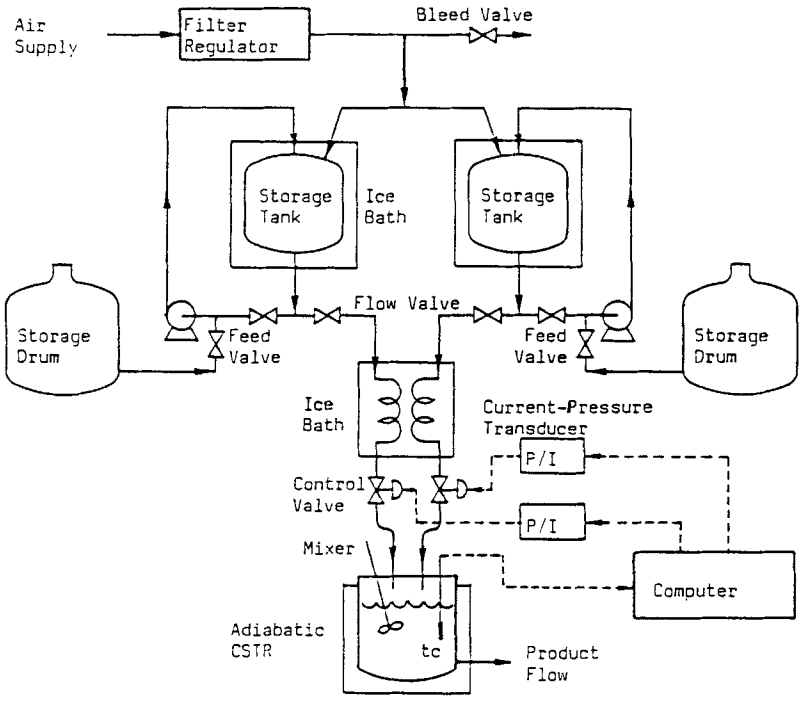

Figure 1. Diagram of experimental reactor system.

tants leaving the storage tanks pass through coiled aluminum tubes inserted in an ice bath and then enter the reactor after going through the automatic control valves. The reactor is made of a polymethylpentene jar 116.8 mm OD × 137.2 mm high, inserted in a wider jar, 133.4 mm OD × 190.5 mm high, to reduce heat losses to the surroundings. The material flows out of the reactor through a large-diameter pipe section inserted in the reactor. The total volume of the reacting material is fixed by adjusting the height of the outlet pipe inside the reactor. For the flow rates and residence times used in the experiments, this arrangement gave satisfactory results for the constant-reacting material volume assumption. A five-channel Doric Trendicator unit with analog output was used to monitor temperatures at the exit of storage tanks, at the exit of the ice bath, and in the reactor. To regulate the feed flow rates two ¼ in. (6.4 mm) stainless steel Research Control automatic control valves are used. The control signals are generated by the computer, converted to 0–10 VDC analog signals and then to 4–20 mA current signals. The current signals are converted to a 20.7–103.4 kPa (3–15 psig) air signal and sent to the actuator of the valve.

The experimental conditions are listed in the righthand column of Table 1. The reactants in all of the experimental runs were prepared using 35 vol. % technical grade hydrogen peroxide and technical grade hypo rice crystal form of sodium thiosulfate.

A Model of the CSTR with Stationary Inputs

Theory

Under conditions of adiabatic operation and perfect mixing, the material and energy balances describing the performance of the CSTR are:

$$\begin{aligned} V(dc_A/dt') &= F(c_{Af} - c_A) \\ &\quad - Vk_0c_Ac_B \exp(-E/RT) \\ V(dc_B/dt') &= F(c_{Bf} - c_B) \\ &\quad - \frac{1}{2} Vk_0c_Ac_B \exp(-E/RT) \\ (m_rc_r + \rho c_PV)(dT/dt') &= \rho c_PF(T_f - T) + (-\Delta H) \\ &\quad \cdot Vk_0c_Ac_B \exp(-E/RT) \end{aligned} \tag{1}$$

where c_A and c_B denote the H_2O_2 and $Na_2S_2O_2$ concentrations, respectively, and b denotes the ratio of the stoichiometric coefficients of the reactants ($b = 2/4 = 0.5$). The term m_rc_r accounts for the total heat capacity of the solid material in contact with the reaction mixture. It is assumed that thermal equilibrium exists between the reacting fluid and the solid material at all times. For stationary inputs or inputs with balanced oscillations, following Chang and Schmitz (1975a), the material balance for c_B can be deleted from the basic system of Eq. 1 since the concentration c_B can be related stoichiometrically to the dimensionless H_2O_2 conversion. Defining the dimensionless concentrations and temperature as

$$x_1 = (c_{Af} - c_A)/c_{Af}, \quad x_{1B} = (c_{Bf} - c_B)/c_{Bf},$$
$$x_2 = [(T - T_f)/T_f](E/RT_f),$$

c_B can be represented as

$$c_B = c_{Bf}(1 - bpx_1),$$

and the dimensionless system equations become:

$$\begin{aligned} dx_1/dt &= -x_1 + Da(1 - x_1)(1 - bpx_1) \\ &\quad \exp[x_2/(1 + x_2/\gamma)] \\ dx_2/dt &= -\lambda x_2 + BDa(1 - x_1) \\ &\quad \cdot (1 - bpx_1) \exp[x_2/(1 + x_2/\gamma)]. \end{aligned} \tag{2}$$

The dimensionless variables used are defined in the Notation. To simplify the calculations, the system equations are reduced to

$$\begin{aligned} dx_1/dt &= -x_1 + Da(1 - x_1)(1 - bpx_1) \exp(x_2Q_1), \\ dx_2/dt &= -\lambda x_2 + BDa(1 - x_1)(1 - bpx_1) \exp(x_2Q_1), \end{aligned} \tag{3}$$

where

$$1/(1 + x_2/\gamma) = \sum_{n=0}^{\infty} (-x_2/\gamma)^n \cong 1 - x_2/\gamma + x_2^2/\gamma^2 \triangleq Q_1$$

since $x_2/\gamma \ll 1$.

The steady states, x_{1s} and x_{2s}, of Eq. 3 are given by

$$\begin{aligned} x_{1s} &= \lambda x_{2s}/B \\ Da &= x_{1s} \exp(-x_{2s}Q_{1s}/[(1 - x_{1s})(1 - bpx_{1s})]. \end{aligned} \tag{4}$$

The necessary and sufficient condition for the existence of multiple steady states for a fixed set of parameters is that the derivative dDa/dx_{1s} be negative over some range of x_{1s}. The local stability analysis can be made utilizing the linearized model equations. Linearizing Eq. 3 around a steady state x_{1s}, x_{2s} and expressing the result in terms of the deviation variables

Table 1. Numerical Values of Parameters and Constants, Operating Conditions

Simulation Studies	Experiments
$C_{Af} = 1.2 \times 10^3$ mol/m^3	$C_{Af} = 1.2 \times 10^3$ mol/m^3
$C_{Bf} = 0.8 \times 10^3$ mol/m^3	$C_{Bf} = 0.8 \times 10^3$ mol/m^3
$k_o = 3.26 \times 10^{13}$ m^3/mol $H_2O_2 \cdot$ s	$T_f = 273.75$ K ± 0.4 K
$-\Delta H/\rho C_p = 73.2 \times 10^3$ m$^3 \cdot$ K/mol	$V = 240$ cm^3
$E = 16.17$ kcal/mol H_2O_2	$F_{max} = 50.7$ cm^3/s
$T_f = 274.1$ K	$F_{min} = 3.0$ cm^3/s
$\xi = 0.1$	Air pressure = 172.4 kPa

$\delta x_1 = x_1 - x_{1s}$, $\delta x_2 = x_2 - x_{2s}$, we obtain

$$\begin{bmatrix} \delta\dot{x}_1 \\ \delta\dot{x}_2 \end{bmatrix} = \begin{bmatrix} \dfrac{2bpx_{1s}^2 - (2+bp)x_{1s}}{(1-x_{1s})(1-bpx_{1s})} & Q_2 x_{1s} \\ \dfrac{Bx_{1s}(2bpx_{1s} - 1 + bp)}{(1-x_{1s})(1-bpx_{1s})} & Q_2 Bx_{1s} - \lambda \end{bmatrix} \begin{bmatrix} \delta x_1 \\ \delta x_2 \end{bmatrix}, \quad (5)$$

where $Q_2 \triangleq 1 - 2x_{2s}/\gamma + 3x_{2s}^2/\gamma^2$. Denoting the coefficient matrix of Eq. 5 by A, the necessary and sufficient conditions for local stability of Eq. 5 are:

$$\text{Det}\, A > 0, \quad \text{tr}\, A < 0.$$

The determinant and the trace of A are

$$\text{Det}\, A = \{-Q_2 Bbpx_{1s}^3 + [Q_2 B(1+bp) - \lambda bp]x_{1s}^2 - Q_2 Bx_{1s} + \lambda\}/[(1-x_{1s})(1-bpx_{1s})] \quad (6)$$

$$\text{tr}\, A = bpx_{1s}^2 - 1/(1-x_{1s})(1-bpx_{1s}) + Q_2 Bx_{1s} - \lambda. \quad (7)$$

A detailed local stability analysis for the hydrogen peroxide-sodium thiosulfate reaction in a CSTR is presented in Schmitz et al. (1979) using the theory developed by Uppal et al. (1974, 1976). For the S-shaped curve defined by Eq. 4, it has been shown that the determinant unstable region corresponds to the negative slope part and, for some parameter values, sections of the positive slope parts may become trace-unstable. Under the experimental conditions used in the present work, there was no trace instability region.

Experimental verification

The parameters of model Eq. 3 are listed in the lefthand column of Table 1. In order to guarantee the qualitative adequacy of this model, two variables have been given special attention: the speed of the mixer and the reactant inlet temperature. An impeller speed of 3.5 rev/s was needed to assure complete mixing. Reactant temperatures had to be monitored at the exit of the feed storage tanks and at the inlet of the automatic control valves to ensure uniform temperatures during the course of an experiment.

The jacket around the reactor was very effective in reducing the heat loss to the surroundings even without vacuum between the reactor and the jacket. In particular, during stabilized periodic operation the heat loss was of little influence. Consequently, adiabatic operation of the reactor was a proper assumption.

Given these measures, both the steady state and the transient behavior of model Eq. 3 have been compared with experimental data. The steady state behavior has been analyzed by comparing the predicted and the experimental steady state temperatures. The results are shown in Figure 2. The agreement is comparable to that observed in earlier studies (Vejsata and Schmitz, 1970; Chang and Schmitz, 1975 a, b).

The transient behavior has been analyzed using step inputs, Figure 3, and periodic inputs. The goal of these experiments was to choose the value of parameter $\xi(=m_r c_r/\rho c_P V)$ so that the transients of Eq. 3 and the reactor were close to each other for the step and periodic inputs. It has been found that there is no

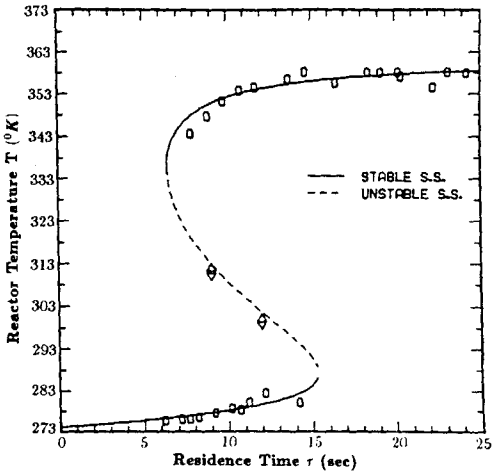

Figure 2. Steady state reactor temperature as a function of residence time.

single value of ξ satisfactory for all temperatures and residence times. However, for a step change from 26.67 to 10.91 cm^3/s in the total feed flow rate (corresponding to a change in τ from 9 to 22 s), a value of $\xi = 0.10$ gave a good fit, Figure 3. For the region of interest in this study, $\xi = 0.10$ gave good results as displayed in the predicted and measured responses to periodic vibrations in reactant input flow rates. This value has been used in model Eq. 3.

A Model of the CSTR with Oscillating Input Flow

Assume that the feed rate is changing according to the law

$$F(t') = F_0[1 + Af(\omega' t')]. \quad (8)$$

Here F_0 is the average flow rate, A is the amplitude, and $f(\omega' t')$ is a periodic zero mean function with frequency ω'.

The function $f(\omega' t')$ may have different shapes, such as sinusoidal, square wave, or nonsymmetric rectangular. For linear systems the optimal shape of oscillations is a nonsymmetric rectangular wave form (Meerkov, 1980).

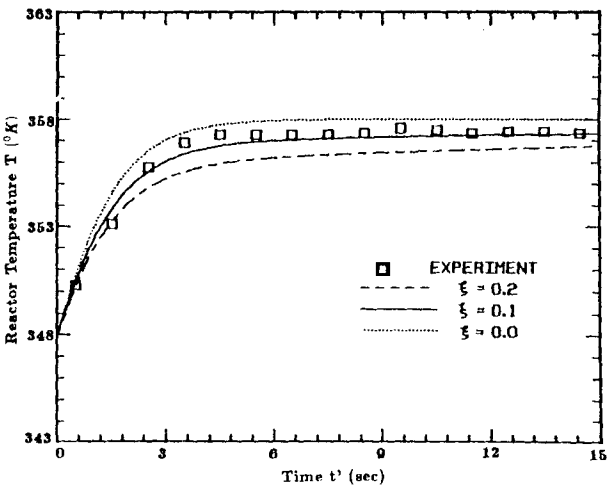

Figure 3. Change in reactor temperature as a response to a step change in feed flow rate.

Assuming that the volume of the reaction mixture is kept constant, the material and energy balances are of the form

$$Vdc_A/dt' = F_0[1 + Af(\omega' t')](c_{Af} - c_A) - Vk_0 c_A c_B \exp(-E/RT)$$

$$(m_r c_r + \rho c_P V)dT/dt' = \rho c_P F_0[1 + Af(\omega' t')](T - T_f) + (-\Delta H)Vk_0 c_A c_B \exp(-E/RT). \quad (9)$$

Using the dimensionless frequency $\omega = \omega'\tau$, the simplified dimensionless equations can be written as

$$dx_1/dt = -[1 + Af(\omega t)]x_1 + Da(1 - x_1) \cdot (1 - bpx_1)\exp(x_2 Q_1)$$

$$dx_2/dt = -\lambda[1 + Af(\omega t)]x_2 + BDa(1 - x_1) \cdot (1 - bpx_1)\exp(x_2 Q_1). \quad (10)$$

Let T_r be the dimensionless characteristic response time of the system with stationary inputs. Choose the dimensionless frequency to satisfy the inequality $\omega \gg (1/T_r)$. Then, introducing the notations

$$\epsilon = \frac{1}{T_r \omega} \ll 1$$

$$A = \frac{\alpha}{\epsilon T_r} \quad (11)$$

Eq. 10 can be rewritten as

$$dx_1/dt = -[1 + (\alpha/\epsilon T_r) f(t/\epsilon T_r)]x_1 + Da(1 - x_1)(1 - bpx_1)\exp(x_2 Q_1)$$

$$dx_2/dt = -\lambda[1 + (\alpha/\epsilon T_r) f(t/\epsilon T_r)]x_2 + BDa(1 - x_1)(1 - bpx_1)\exp(x_2 Q_1), \quad (12)$$

where the vibrations are of the form of Eq. A2, given in the Appendix.

Finding an analytical solution of these equations, where $f(\cdot)$ is a periodic function, is a formidable task. Vibrational control theory offers a method of analysis to circumvent this difficulty. This method of analysis, summarized in the Appendix, is applied below to the CSTR model equations to investigate the behavior of the CSTR under oscillating input flow rates.

Asymptotic Analysis

The CSTR model equations with oscillating input flow rate, Eq. 12, are of the form of Eq. A3 (Appendix) with

$$X_1(x) = \begin{bmatrix} -x_1 + Da(1 - x_1)(1 - bpx_1)\exp(x_2 Q_1) \\ -\lambda x_2 + BDa(1 - x_1)(1 - bpx_1)\exp(x_2 Q_1) \end{bmatrix} \quad (13)$$

Therefore, the property of vibrational stabilizability of x_s follows from the property of asymptotic stability of the equilibrium position z_s of the averaged system equations of the form of Eq. A10. To obtain the averaged system equations, introduce the generating equations of the form of Eq. A5 with

$$X_2\left(\frac{t}{\epsilon}, x\right) = -\sum_{k=1}^{n} \alpha_k \cos(k\omega t)\begin{bmatrix} x_1 \\ \lambda x_2 \end{bmatrix}. \quad (14)$$

The resulting system in the standard form, Eq. A8, in the fast time $\theta = t/\epsilon$ is:

$$dy_1/d\theta = -\epsilon y_1 + \epsilon Da\{\exp[g(\theta)] - bpy_1 + bpy_1^2 \exp[-g(\theta)]\} \exp\{y_2 \exp[-\lambda g(\theta)] - y_2^2 \exp[-2\lambda g(\theta)]/\gamma + y_2^3 \exp[-3\lambda g(\theta)]/\gamma^2\}$$

$$dy_2/d\theta = -\epsilon\lambda y_2 + \epsilon BDa\{\exp[g(\theta)] - bpy_1 + bpy_1^2 \exp[-g(\theta)]\} \exp\{y_2 \exp[-\lambda g(\theta)] - y_2^2 \exp[-2\lambda g(\theta)]/\gamma + y_2^3 \exp[-3\lambda g(\theta)]/\gamma^2\} \quad (15)$$

where

$$g(\theta) = \sum_{k=1}^{n} (\alpha_k/k)\sin(k\theta).$$

The averaged equations, Eq. A10, are

$$dz_1/dt = -z_1 + Da((1 - z_1)(1 - bpz_1) + \mu^2\{1 + \lambda^2(F_2 + F_1^2) - 2\lambda F_1 - \lambda^2(F_2 + F_1^2)(1 + bp)z_1 + bp[1 + \lambda(2F_1 + \lambda F_2 + \lambda F_1^2)]z_1^2\})\exp(F_0)$$

$$dz_2/dt = -\lambda z_2 + BDa((1 - z_1)(1 - bpz_1) + \mu^2\{\lambda^2(1 + F_2 + F_1^2 - 2F_1) - [(\lambda - 1)^2 + \lambda^2 F_2 + (\lambda F_1)^2 - 2\lambda(\lambda - 1)F_1] \cdot z_1(1 + bp) + bp[(\lambda - 2)^2 + 2(2 - \lambda)\lambda F_1 + \lambda^2 F_2 + \lambda^2 F_1^2]z_1^2\})\exp(F_0), \quad (16)$$

where

$$F_0 = z_2(1 - z_2/\gamma + z_2^2/\gamma^2)$$

$$F_1 = z_2(1 - 2z_2/\gamma + 3z_2^2/\gamma^2)$$

$$F_2 = z_2(1 - 4z_2/\gamma + 9z_2^2/\gamma^2)$$

The expression for μ varies with the type of periodic function used for oscillating the input flow rates. For a sinusoidal periodic function with amplitude A and frequency ω,

$$\mu^2 = A^2/4\omega^2. \quad (17)$$

For a symmetric square wave function with amplitude A and frequency ω,

$$\mu^2 \simeq (1/4\omega^2)\sum_{k=0}^{n} 16A^2/(2k + 1)^2\pi^2, \quad (18)$$

For a nonsymmetric rectangular zero average wave form

$$\mu^2 \simeq [(Da_{max} - Da_{min})^2 Da^2/(\pi^2 Da_{min}^2 Da_{max}^2 \omega^2)] \cdot \sum_{k=1}^{n} (1/k^4) \sin^2 [k\pi Da_{min} (Da_{max} - Da)/Da(Da_{max} - Da_{min})], \quad (19)$$

where Da_{min} and Da_{max} are computed using, respectively, τ_{max} and τ_{min} due to oscillations in the input flow rates. In this study, n was chosen to be 15 for the symmetric square waveform and to be 30 for the nonsymmetric rectangular waveform.

The averaged Eq. 16 will be used in simulation studies for the selection of bounds on the frequency of flow rate variations.

The steady state characteristics of the averaged system, Eq. 16, are given by

$$\begin{aligned} z_{1s} &= \lambda z_{2s}/B \\ Da &= z_{1s} \exp(-F_{0s})/((1 - z_{1s})(1 - bpz_{1s}) \\ &\quad + \mu^2\{1 + \lambda^2(F_{2s} + F_{1s}^2) - 2\lambda F_{1s} \\ &\quad - \lambda^2(F_{2s} + F_{1s}^2)(1 + bp)z_{1s} \\ &\quad + bp[1 + \lambda(2F_{1s} + \lambda F_{2s} + \lambda F_{1s}^2)]z_{1s}^2\}) \end{aligned} \quad (20)$$

and are shown in Figure 4 for various values of ω. (Note that $\mu = 0$ corresponding to stationary inputs gives the steady state characteristic of the reactor without vibrations, Eq. 3, that has the largest negative slope part.) For all shapes of forcing functions, an increase in frequency or a reduction in amplitude moves the steady state curve with periodic forcing closer to the steady state curve of the system without vibrations. As the value of μ is increased (reduction in ω), the upper stable steady state curve is lowered, creating an opportunity for stable operation in the unstable steady state region of the system. Such an operation would be of interest if the temperature corresponding to the upper steady state of the original system is likely to cause reactant or product disintegration due to high temperature.

To analyze the local stability properties, consider the linear approximation of Eq. 16 around a steady state z_{1s}, z_{2s}:

$$\begin{bmatrix} \delta\dot{z}_1 \\ \delta\dot{z}_2 \end{bmatrix} = \boldsymbol{A}^* \begin{bmatrix} \delta z_1 \\ \delta z_2 \end{bmatrix} \quad (21)$$

where

$$\boldsymbol{A}^* = \begin{bmatrix} A_{11}^* & A_{12}^* \\ A_{21}^* & A_{22}^* \end{bmatrix}. \quad (22)$$

Here

$$\begin{aligned} A_{11}^* &= -1 + Da\{2bpz_{1s} - (1 + bp) \\ &\quad + \mu^2[-(1 + bp)\lambda^2(F_{2s} + F_{1s}^2) \\ &\quad + 2bpz_{1s}(\lambda^2 F_{2s} + \lambda^2 F_{1s}^2 + 2\lambda F_{1s} + 1)]\} \exp(F_{0s}) \\ A_{12}^* &= F_0' Da((1 - z_{1s})(1 - bpz_{1s}) \\ &\quad + \mu^2\{\lambda^2(F_{2s}' + 2F_{1s}F_{1s}') - 2\lambda F_{1s}' \\ &\quad - (1 + bp)z_{1s}\lambda^2(F_{2s}' + 2) + bpz_{1s}^2(\lambda^2 F_{2s}' \\ &\quad + 2\lambda^2 F_{1s}F_{1s}' + 2\lambda F_{1s}' + F_{0s}'[1 + \lambda^2 F_{2s} + \lambda^2 F_{1s} - 2\lambda F_{1s} \\ &\quad - (1 + bp)z_{1s}\lambda^2(F_{2s} + F_{1s}^2) + bpz_{1s}^2(\lambda^2 F_{2s} + \lambda^2 F_{1s}^2 \\ &\quad + 2\lambda F_{1s} + 1)]\} \exp(F_{0s}) \\ A_{21}^* &= BDa(2bpz_{1s} - (1 + bp) \\ &\quad + \mu^2\{-(1 + bp)(\lambda - 1)^2 + \lambda^2 F_{2s} \\ &\quad + \lambda^2 F_{1s}^2 + 2\lambda(\lambda - 1)F_{1s} + 2bpz_{1s}[(\lambda - 2)^2 + \lambda^2 F_{2s} \\ &\quad + \lambda^2 F_{1s}^2 + 2(2 - \lambda)\lambda F_{1s}]\}) \exp(F_{0s}) \\ A_{22}^* &= -\lambda + BDa((1 - bpz_{1s})(1 - z_{1s})F_{0s}' \\ &\quad + \mu^2\{F_{0s}'[\lambda^2(1 + F_{2s} + F_{1s}^2 - 2F_{1s}) \\ &\quad - (1 + bp)z_{1s}][(\lambda - 1)^2 + \lambda^2 F_{2s} \\ &\quad + \lambda^2 F_{1s}^2 - 2\lambda(\lambda - 1)F_{1s}] + bpz_{1s}^2[(\lambda - 2)^2 \\ &\quad + \lambda^2(F_{2s} + F_{1s}^2) + 2\lambda(2 - \lambda)F_{1s})] \\ &\quad + \lambda^2(F_{1s}' + 2F_{1s}F_{1s}' - 2F_{1s}') \\ &\quad - (1 + bp)z_{1s}[\lambda^2(F_{2s}' + 2F_{1s}F_{1s}') \\ &\quad - 2\lambda(\lambda - 1)F_{1s}'] + bpz_{1s}^2[\lambda^2(F_{2s}' + 2F_{1s}F_{1s}') \\ &\quad + 2(2 - \lambda)\lambda F_{1s}']\}) \exp(F_{0s}) \end{aligned}$$

where

$$\begin{aligned} F_{0s} &= z_{2s}(1 - z_{2s}/\gamma + z_{2s}^2/\gamma^2) \\ F_{1s} &= z_{2s}(1 - 2z_{2s}/\gamma + 3z_{2s}^2/\gamma^2) \\ F_{2s} &= z_{2s}(1 - 4z_{2s}/\gamma + 9z_{2s}^2/\gamma^2) \\ F_{0s}' &= 1 - 2z_{2s}/\gamma + 3z_{2s}^2/\gamma^2 \\ F_{1s}' &= 1 - 4z_{2s}/\gamma + 9z_{2s}^2/\gamma^2 \\ F_{2s}' &= 1 - 8z_{2s}/\gamma + 27z_{2s}^2/\gamma^2 \end{aligned}$$

Analyzing the *Det* $\boldsymbol{A}^*$ and *tr* $\boldsymbol{A}^*$ it is possible to show that *tr* $\boldsymbol{A}^* < 0$ for every steady state of the reactor defined by the parameters in Table 1, and *Det* $\boldsymbol{A}^* > 0$ for all but the steady states on the negative slope part of the *S*-shaped curve. Thus, introduction of oscillations causes a decrease in the unstable domain of the steady state curve.

Bounds on Frequencies and Amplitudes

Under stabilized periodic operation, for a given type of input function, the deviations of the output variables from their average values depend on the frequency and amplitude of oscillations in the input variables. As will be discussed in detail later, increases in amplitude result in large deviations of the output variables from their average values. Increases in frequency have an opposite effect. Furthermore, increases in amplitude move the average stabilized state away from the upper stable steady state of the system with stationary inputs, whereas increases in frequency bring them closer. Consequently, proper selection of the amplitude and frequency is crucial in maintaining the stabilized periodic operation around a desired average state with deviations of acceptable magnitude.

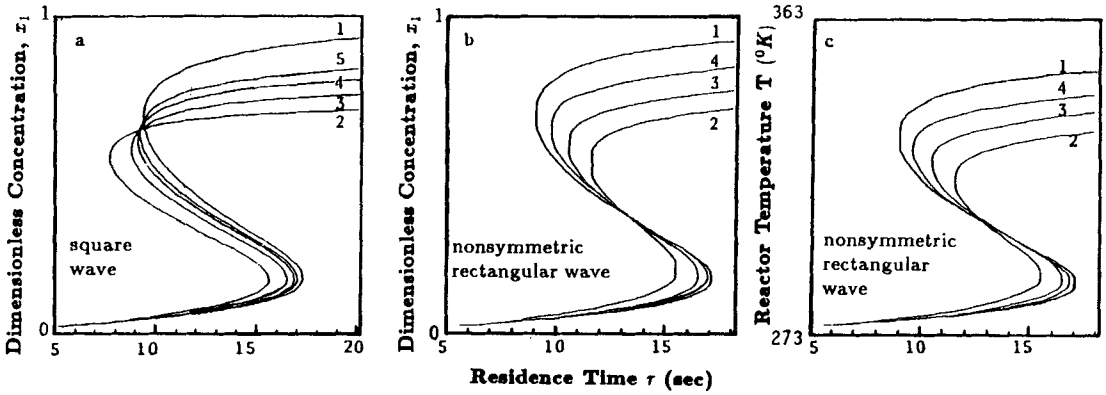

Figure 4. Average steady state characteristics of CSTR with periodic forcing of input flow rates.
1, stationary inputs; 2, $\omega = 1$; 3, $\omega = 2$; 4, $\omega = 3$; 5, $\omega = 4$

Another area of concern is to find a lower bound for the frequency region in which vibrational control and the asymptotic analysis will be valid. The upper bound is less critical. Too high a frequency will make the periodic variations in inputs look like noise and the capacity of the system will filter out their effect. From a practical point of view there is no need to increase the frequency to a higher value if a lower frequency is satisfactory. Unnecessary increases in frequency will result in excessive use of the final control elements (the control valves in this case) and may also be limited by their dynamics.

The lower bound on the frequency is computed by estimating the maximum acceptable value for ϵ, ϵ_{max}. Recalling Proposition 2 of the Appendix, for a given δ_0 an $\epsilon_{max}(\delta)$ can be found such that $\| \bar{x}(t) - z(t) \| \leq \delta_0$ for $\epsilon \leq \epsilon_{max}$. The opposite is also true: for a given ϵ, $\bar{x}$ and z may be computed from the model equations and the corresponding δ can be calculated. Repeating the computations for various values of ϵ, a relationship can be formulated between ϵ and δ and a plot of δ vs. ϵ can be made with amplitude of the input signal as a parameter. Then selecting the acceptable value of δ_0, the corresponding ϵ_{max} can be found. Since the frequency is $\omega = 1/T_r\epsilon$, the lower bound of ω can be computed for a given value of τ and T_r.

The time constant T_r as a function of the residence time τ is computed from the transient model equations and plotted in Figure 5 for the upper and lower regions of operation. Using transient simulations, the error function $\delta(\epsilon, A)$ is computed for various values of ϵ and A. Curves are presented for the upper and lower regions of operation with single and multiple steady states in Figure 6 for specific values of τ. For example for $\tau = 14$ s in the upper region of operation $T_r = 0.57$. If a δ of 0.1 (or 10%) is acceptable, for a square wave input of $A = 0.9$, $\epsilon_{max} = 0.75$. Consequently the lower bound on ω is $\omega = 1/\epsilon_{max} T_r = 1/(0.75)(0.57) = 2.34$.

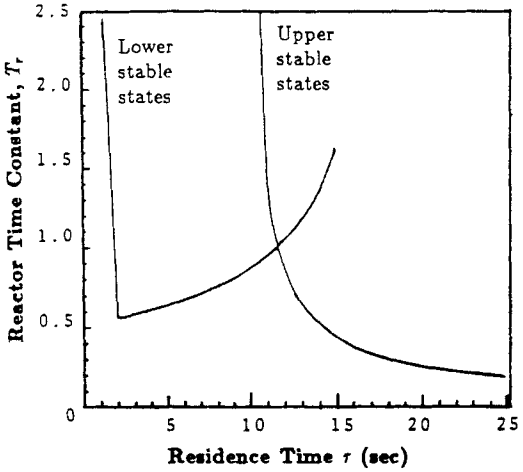

Figure 5. Reactor time constant T_r as a function of residence time.

Simulation Results

To verify the above analytical predictions, numerical simulation studies have been carried out. The trajectories of the system with vibrations, Eq. 12, have been compared with solutions of the averaged Eq. 16. The results are shown in Figures 7 and 8 for $Da = 0.08$ and square wave forcing. In Figure 7 the effect of

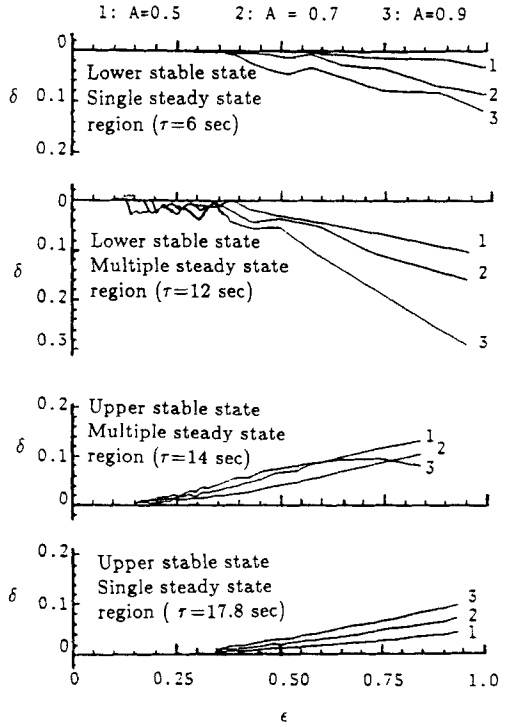

Figure 6. Effect of ϵ on δ.

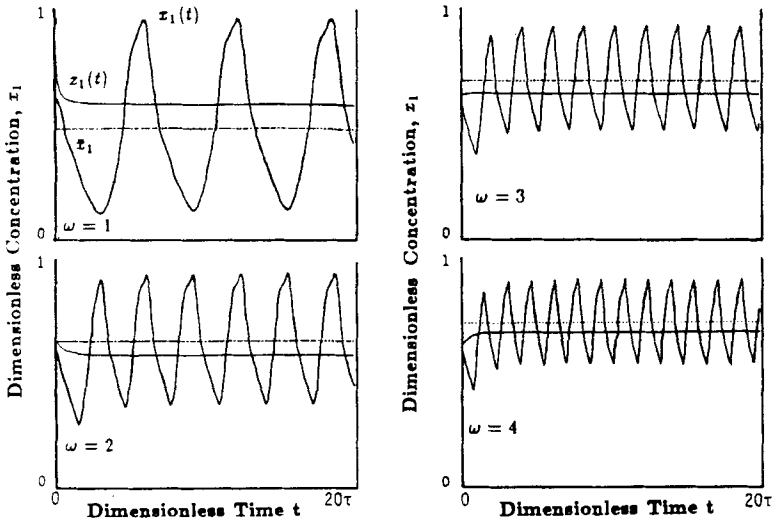

Figure 7. Fractional H_2O_2 conversion as a function of variations in frequency of flow rate oscillations.
Square wave input forcing, upper stable state.
$Da = 0.08$, $B = 8.0$, $bp = 0.75$, $A = 0.9$

varying the frequency (or ϵ) at constant amplitude ($A = 0.9$) is displayed. As predicted, with increasing frequency (or decreasing ϵ) the precision of the averaged description improves, i.e., the difference between the average value of the stabilized state and the value of z decreases. Also with increasing frequency, the value of the averaged steady state approaches the value of the state with stationary inputs, and the amplitude of oscillation of the stabilized state is reduced. The effect of amplitude on the average of the stabilized state and on the averaged state for a fixed value of frequency is given in Figure 8. A reduction in amplitude has an effect similar to an increase in frequency.

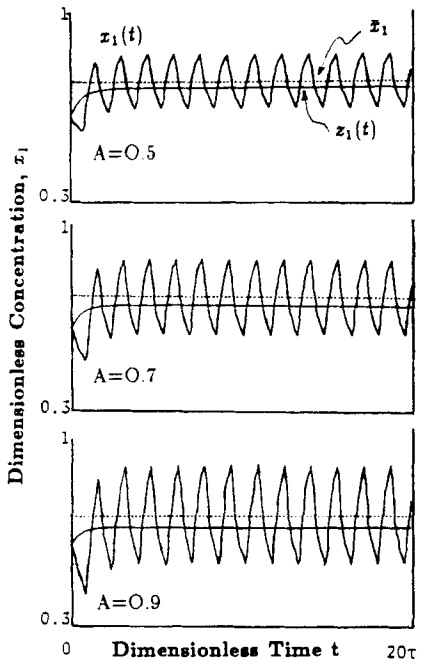

Figure 8. Fractional H_2O_2 conversion as a function of variations in amplitude of flow rate oscillation.
Square wave input forcing, upper stable steady state.
$Da = 0.08$, $B = 8.0$, $bp = 0.75$, $\omega = 4$

The vibrational stabilization achieved is due to the fact that an asymptotically stable limit cycle is organized instead of the unstable steady states of the system with stationary inputs, in such a manner that the average temperature along this limit cycle is arbitrarily close to the temperature of the original (stationary-input system) unstable state.

For a given state, the average residence time under vibrational control operation may be different than the residence time of the system with fixed inputs. The proximity of the two residence times depends on factors such as the amplitude and frequency of the forced input variation, the shape of the forcing function, and the input variable vibrated. The two residence times will coincide if the average steady state curve has a positive slope at the point of intersection with the negative slope part of the curve for the fixed-input system. In Figure 4a the intersections of curves 1 and 3 or curves 1 and 2 illustrate cases where for a given state the two residence times coincide.

Although the average temperatures of the stabilized states are lower than the temperature of the upper steady state for a given residence time, the peak temperatures approach the upper steady state temperature, Figures 7 and 8. However, the duration of these high temperatures within one period of oscillation is small. For a given input amplitude, the fraction of time duration at high temperatures and the amplitude of oscillation are inversely proportional to the frequency of oscillation, Figure 7. By reducing the amplitude of input vibrations and increasing frequency, the peak temperatures can be lowered and the duration of high temperatures can be reduced to tolerable levels. Another approach for reducing the maximum temperature is simultaneous vibrations in two input variables. The results achieved by this approach will be reported in a future publication.

Experimental Studies

Experiments have been conducted in order to verify the stability of the averaged steady (stabilized) states obtained by forced periodic variations in inlet flow rates as predicted by theoretical studies and simulations. Furthermore, the effect of oscillation frequency on the location of the averaged states and on the

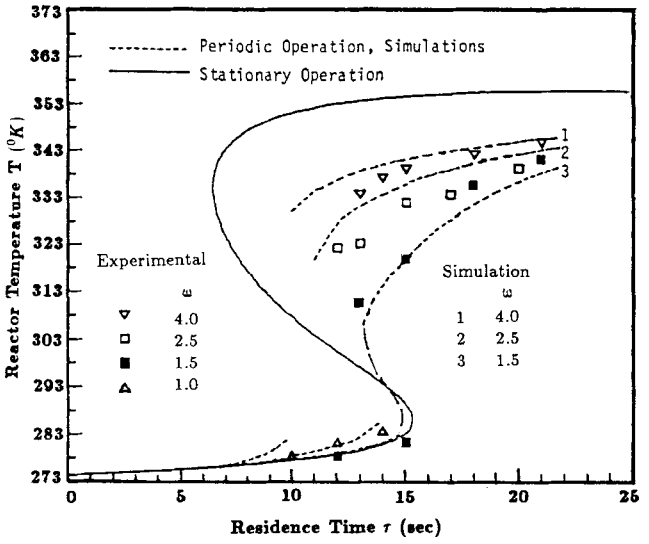

Figure 9. Steady state characteristics of experimental CSTR system with and without vibrational control.

shape and amplitude of the stabilized oscillations in reactor temperature has been studied. In Figures 10–13 various plots are presented showing the dynamic behavior of the reactor system when operated under vibrational control and when input oscillations are discontinued.

In all experiments nonsymmetric rectangular waveforms have been used. The maximum and minimum valve openings are 80 and 5%, corresponding to 23.5 cm^3/s and 1.6 cm^3/s for each stream. The operating conditions are given in the righthand column of Table 1. The value of the average flow rate has been fixed by the residence time value selected for an experimental run.

Verification of steady state behavior

The loci of the averaged stabilized reactor temperatures for various values of the frequency of oscillations in input flow rates are given in Figure 9. The experimental steady states indicated are obtained by averaging the stabilized reactor temperatures under vibrational operation such as that shown in Figures 10–12. The shapes and relative locations of the experimental steady state curves on the $(T - \tau)$ plane agree well with the theoretical steady state curves, Figure 4. The upper branch of the steady state curve is lower in vibrational operation and the lower branch of the steady state curve is higher than the steady state curve of the stationary system. As the frequency of the input oscillations is reduced, both branches of the curve move away from the stationary operation curve. Hence vibrational operation on the lower branch can be used to increase conversion and vibrational operation on the upper branch can be used to limit temperature increases in the reactor.

Under vibrational control, the negative slope part of the steady state curve is reduced and the negative slope itself is increased. Although for the range of experimental conditions used in this study the negative slope part is not eliminated, the trend observed indicates that for some conditions the elimination of the negative slope part of the curve would be possible. The changes in the location of the ignition and extinction points follow the theoretical predictions: the ignition point moves to the left and the extinction point to the right. In the multiple steady state region, as the residence time is decreased the extinction of the reaction takes place at $\tau = 9$ s for $\omega = 4.0$. As predicted, this value of τ is higher than the extinction point of the reactor system with stationary inputs ($\tau = 6.5$ s).

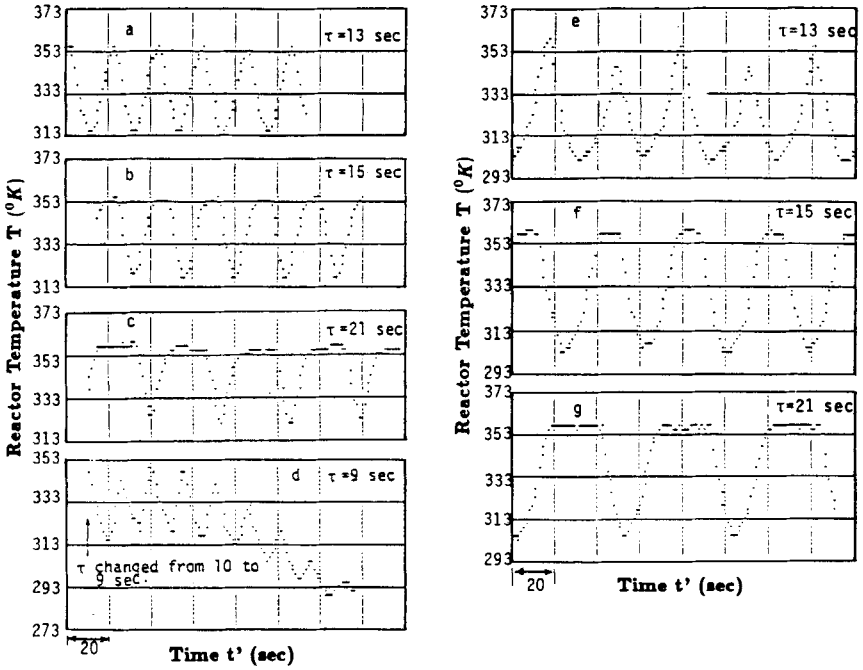

Figure 10. Variations in temperature of CSTR under vibrational control.
a, b, c, d, $\omega = 4.0$; e, f, g, $\omega = 2.5$
Upper stabilized state

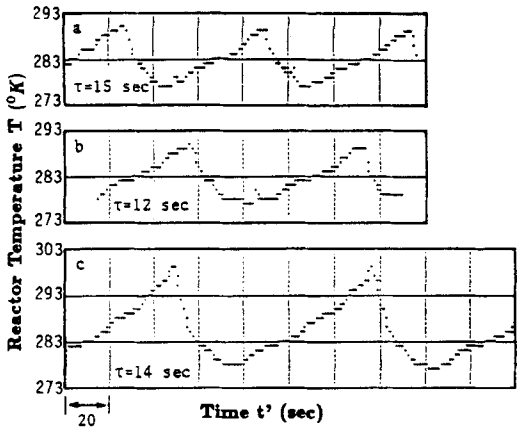

Figure 11. Variations in temperature of CSTR under vibrational control.

a, $\omega = 1.5$; b, c, $\omega = 1.0$
Lower stabilized state

The experimental results verify the theoretical predictions that vibrational control enables stable periodic operation that would become unstable when there are no oscillations in the input flow rates. In experiments conducted in the multiple steady state region, if after stabilized operation is reached the input vibrations are discontinued, the reaction temperature migrates to the stationary steady state temperature, Figure 13.

Effect of oscillation frequency and amplitude

The effect of the frequency of flow oscillations on the reactor temperature is given in Figures 10–12. For various values of

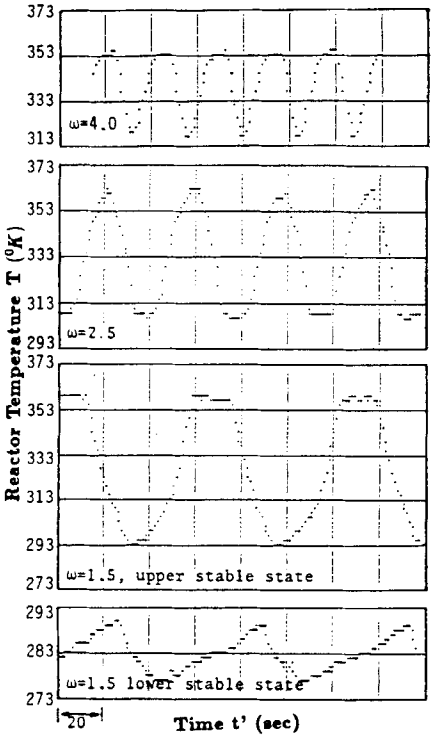

Figure 12. Variations in temperature of CSTR under vibrational control.

Residence time $\tau = 15$ s

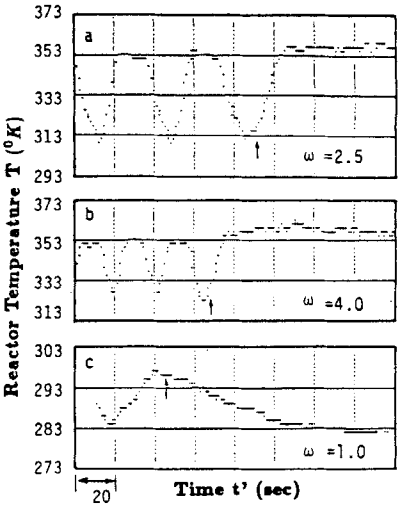

Figure 13. Reactor temperature transients when oscillations in feed flow rate are discontinued.

Residence time $\tau = 14$ s. Feed flow rate adjusted to average value at time indicated by ↑.

reactor residence time, oscillations in reactor temperature are shown in Figure 10 for $\omega = 4.0$ and 2.5, for the upper stable averaged state. For the lower stable averaged state, Figure 11 illustrates the temperature variations for $\omega = 1$ and 1.5. Since the reactor time constant is larger at the lower stable states, smaller frequencies can be used. In Figure 12 the reactor temperatures for various values of ω are shown for $\tau = 15$ s. For different values of τ and ω, the average and the peak reactor temperatures are listed in Table 2. As predicted, the peak temperature decreases and the average temperature increases with an increase in the frequency of input oscillations.

The experimental results indicate that the frequency ranges selected by the algorithm proposed in this work give satisfactory results. In the upper steady state region, as the frequency of

Table 2. Summary of Experimental Results

Residence Time, τ s	Freq. ω	Period $2\pi\tau/\omega$ s	Avg. Temp. K	Peak Temp. K
21	4.0	33.0	347.0	358.7
18	4.0	28.3	344.0	355.2
15	4.0	23.6	340.5	354.6
14	4.0	22.0	338.5	356.5
13	4.0	20.4	335.0	355.7
12	4.0	18.9	328.7	352.7
20	2.5	50.3	341.4	357.0
17	2.5	42.7	335.5	357.9
15	2.5	37.7	333.5	359.8
13	2.5	32.7	324.5	358.3
12	2.5	30.2	323.5	358.4
21	1.5	88.0	343.5	361.8
18	1.5	75.4	337.5	358.8
15	1.5	62.8	321.5	358.0
15	1.5	62.8	282.5	290.0
13	1.5	54.5	311.9	358.8
14	1.0	88.0	285.1	299.4
12	1.0	75.4	282.4	289.6
15	0	∞	356.8	—

input vibrations is reduced below 2.5 the reactor temperature oscillates between the upper and lower stationary steady state temperatures in a quasi-steady state fashion, indicating that the oscillation frequency is too low to satisfy the conditions of vibrational control.

In all experiments reported in various figures the maximum possible amplitude was used. For the nonsymmetric rectangular waveform, during a fraction of the period each valve was opened 80%, then the valve opening was reduced to 5%. The length of each time fraction was selected based on the average residence time. In experiments conducted with smaller amplitudes the averaged stabilized states were closer to the stationary steady states, confirming the theoretical predictions. Since the effects of vibrational control are stronger at high amplitudes, in the experiments the highest possible vibration amplitudes are used.

Verification of the dynamic behavior

With oscillatory flow rates, the peak temperatures in the reactor are close to the steady state temperatures of the system with stationary input flows. However, at a given frequency, the fraction of the time (in a period) during which the peak reactor temperature stays close to the upper steady state temperature is inversely proportional to the feed flow rates, Figures 10–12. This trend agrees with the trend observed in the simulation of oscillations in fractional conversion, Figures 7 and 8. The high flow rates are in the multiple steady state region and correspond to a desired operation policy for the reactor for high productivity. Consequently, the region where the reactor temperature (under vibrational control) stays longer in the vicinity of the averaged stabilized temperature coincides with the operating region with higher productivity and vibrational control becomes a viable option when operation at an unstable steady state is desired.

Trajectories of reactor temperature as the stable periodic operation in the multiple steady state region is stopped by discontinuing the vibrations in the feed flow rate and equating the feed flow rate to its previous averaged value are given in Figure 13. In all cases considered, when the input oscillations are discontinued the reaction temperature migrated to the stable steady state temperature of the system with stationary inputs corresponding to the same region of operation. In other words, if the average temperature of the stabilized state was above the unstable intermediate state temperature of the vibrational system, the reactor temperature attained the upper steady state temperature of the system with stationary inputs. Otherwise, the reactor temperature converged to the lower steady state temperature of the stationary-input system. Consequently, vibrational control introduces new stabilized states that do not exist for the system with stationary inputs under the same operating conditions.

Benefits of Vibrational Control

Vibrational control can be used to reduce the capital and operating costs of exothermic CSTR's that need external cooling. The plots of the averaged values of the stabilized reactor temperatures under vibrational control as a function of residence time are quite similar to the steady state temperature profiles of a reactor with a cooling mechanism (Chang and Schmitz, 1975b, Figures 1, 9). Consequently, vibrational control offers an alternative to operation at a state that is stabilized by feedback control of a coolant flow rate. For example, the cooling water flow rate reported by Chang and Schmitz (1975b) is almost three times the reactant flow rate with a coolant inlet temperature of 273 K and it will be much higher under customary cooling water temperatures used in the industry. The stabilized reactor temperature with their arrangement fluctuates within 4 K. If strict temperature regulation is mandatory, such a cooling mechanism may be needed. If however the constraints on temperature swings can be relaxed and the constraint is imposed on the average temperature of the stabilized state, then vibrational control becomes a viable alternative. Use of vibrational control will eliminate the capital and operating costs related to the cooling system and consequently will result in substantial savings in energy.

Steady state curves passing through an average stabilized operation point of the vibrationally controlled reactor system can be obtained with a system with stationary inputs by varying the value of an input such as the inlet concentration or the inlet temperature, Figure 14. Such an adjustment will have an opportunity cost. If the inlet temperature is lowered, that would cause an increase in cooling costs. If the inlet concentration is lowered, the production rate is lowered. In the case of vibrational control, however, the same effect is generated without such added costs. For example if reactor operation at 338 K is desired, the reduction in feed concentration results in a drop in 28% in production rate with respect to the production under vibrational control (with $\omega = 4.0$).

For systems with costly and difficult measurements or long measurement delays, vibrational control can be used to eliminate such handicaps. Since it is an open-loop control system, it does not require fast, on-line measurements. Off-line measurements can be used to check the status of the system under control and to adjust the oscillation frequency or amplitude, if needed.

The combination of vibrational control with feedback control offers many advantages. Vibrational-plus-feedback (V F) control may be used such that the feedback control commands are kept away from those values that cause saturation of the final control elements. In this case the vibrational controller would be responsible for shifting the control load to prevent saturation, and the feedback controller would be responsible for regulation. Another area of application of VF control is in achieving con-

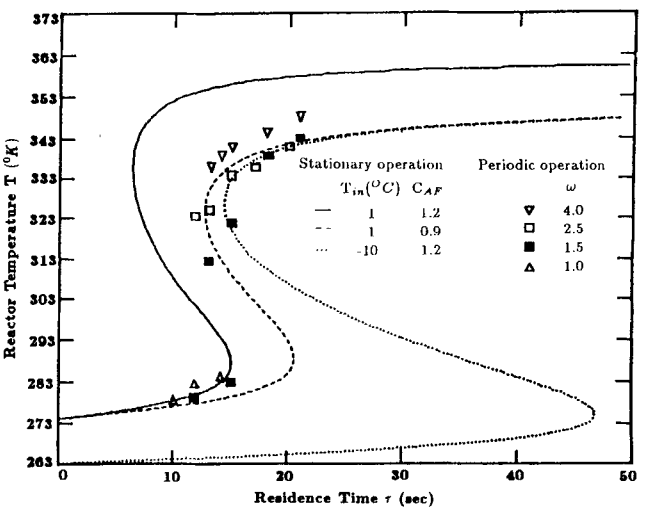

Figure 14. Steady state characteristics of experimental CSTR system with modified inlet conditions.

trollability of an otherwise uncontrollable system by vibrational control and using feedback control to regulate this improved system. The application of VF control to chemical reactor systems will be the topic of a future presentation.

Acknowledgments

The authors are indebted to the U.S. Department of Energy for financial support. Ali Cinar and Jian Deng are supported by DOE under Grant No. DE-FG02-84ER13205, Semyon M. Meerkov and Xianshu Shu are supported by DOE under Grant No. DE-FG02-85ER13315.

Notation

A = amplitude of oscillations in input flow rates
$\boldsymbol{A}, A$ = coefficient matrices, Eqs. 5, 22
b = ratio of stoichiometric coefficients, $Na_2S_2O_3/H_2O_2$
B = dimensionless parameter group, $(-\Delta H)c_{Af}\gamma/\rho c_P T_f(1+\xi)$
c_A, c_B = hydrogen peroxide and sodium thiosulfate concentration, respectively
c_P, c_m = heat capacity of reacting mixture and reactor material
Da = Damkohler number, $c_{Bf}k_o \exp(-\gamma)\tau$
E = activation energy
F, F_0 = feed flow rate and its average value
F_0, F_1, F_2 = defined under Eq. 16
F_{0s}, F_{1s}, F_{2s} = defined under Eq. 22
$F'_{0s}, F'_{1s}, F'_{2s}$ = defined under Eq. 22
ΔH = heat of reaction
k_o = reaction rate constant
p = ratio of feed concentrations, c_{Af}/c_{Bf}
Q_1 = defined under Eq. 3
Q_2 = defined under Eq. 5
R = universal gas constant
t', t = time, and dimensionless time t'/τ
T = reactor temperature
T_f = reactant feed temperature
T_r = reactor rise time
V = volume of reaction mixture
x_1 = dimensionless hydrogen peroxide concentration $(c_{Af} - c_A)/c_{Af}$
x_2 = dimensionless temperature $(T - T_f)\gamma/T_f$
y_1, y_2 = dimensionless H_2O_2 concentration and temperature in the standard form; see Appendix
z_1, z_2 = averaged dimensionless H_2O_2 concentration and temperature in oscillatory operation

Greek letters

α = scalar, Eq. A2
γ = dimensionless activation energy E/RT_f
$\delta(\cdot)$ = deviation variable (from steady state)
ϵ = parameter, Eq. 11
θ = fast time t/ϵ
λ = dimensionless group, $1/(1+\xi)$
μ = amplitude-to-frequency ratios for various types of periodic forcing functions, Eqs. 17–19
ξ = dimensionless parameter group, $m_r c_r/\rho c_P V$
ρ = density of reacting mixture
τ = residence time V/F
ω', ω = frequency and its dimensionless form

Subscripts

f = feed state
s = steady state

Appendix: Method of Analysis

The analysis of a vibrationally controlled system is equivalent, from the mathematical standpoint, to the analysis of a dynamic system with parametric oscillations.

Consider a system of the form:

$$\dot{x} = X(x, \lambda), \quad X: R^n \times R^m \to R^n, \tag{A1}$$

where $x \in R^n$ is the state, t is the dimensionless time, and $\lambda = \lambda(t) \in R^m$ is a fast oscillating parameter. Assume that $\lambda(t)$ is defined by

$$\lambda = \lambda_0 + (\alpha/\epsilon) f(t/\epsilon), \tag{A2}$$

where $\lambda_0 = \text{const}$, $f(\cdot)$ is a periodic or quasi-periodic zero average vector, and $0 < \epsilon \ll 1$ and $0 < \alpha$ are scalars. Assume, finally, that Eq. A1 with λ as in Eq. 2 has the form

$$dx/dt = X_1(x) + (\alpha/\epsilon)X_2(t/\epsilon, x), \qquad X_1: R^n \to R^n; \quad X_2: R_+ \times R^n \to R^n, \tag{A3}$$

where $X_2(t/\epsilon, \cdot)$ is a periodic or quasi-periodic function.

In the fast time $\theta = t/\epsilon$, Eq. A3 can be rewritten as

$$dx/d\theta = \epsilon X_1(x) + \alpha X_2(\theta, x). \tag{A4}$$

Introduce a generating equation

$$dx/d\theta = \alpha X_2(\theta, x). \tag{A5}$$

Assume that there exists a unique solution of Eq. A5 defined by every initial condition $x_0 \in \Omega \subset R^n$ for all $\theta \geq 0$. Denote the general solution of Eq. A5 as

$$x(\theta) = h(\theta, c), \quad c = \text{const} \in \Omega \subset R^n. \tag{A6}$$

Proposition 1. Assume that $X_2(\theta, x)$ is differentiable with respect to x. In this case, a substitution that reduces Eq. A4 to a standard form is

$$x(\theta) = h[\theta, y(\theta)], \quad y \in R^n. \tag{A7}$$

The resulting equation in the standard form is:

$$dy/d\theta = \epsilon[\partial h/\partial y]^{-1} X_1[h(\theta, y)] \triangleq \epsilon Y(\theta, y). \tag{A8}$$

To further analyze Eq. A8, a number of asymptotic (with respect to ϵ) techniques can be employed. Since $dy/d\theta$ is proportional to ϵ whereas $\partial h/\partial\theta \sim 1$, it appears that the averaging principle is advantageous for this purpose. To formulate a general statement with this regard, introduce

$$\lim_{T\to\infty} \frac{1}{T} \int_0^T [\partial h/\partial y]^{-1} X_1[h(\theta, y)]\, d\theta \triangleq Z(y) \tag{A9}$$

and the equation, referred to as the **averaged equation:**

$$dz/d\theta = \epsilon Z(z), \quad z_0 = y_0 \in \Omega \subset R^n. \tag{A10}$$

Proposition 2. Assume that

1. $\| Y(t, y) \| \leq N, \forall t \in (0, \infty), \forall y \in \Omega \subset R^n$;
2. $\| Y(t, y') - Y(t, y'') \| \leq K \| y' - y'' \|, \quad \forall t \in (0, \infty), \forall y', y'' \in \Omega$;
3. Uniformly with respect to $y \in \Omega$, there exists a limit, Eq. A9. Then, for every positive δ and σ as small as desired and L as

large as desired, there exists $\epsilon_0(\delta, L, \sigma)$ such that for each $0 < \epsilon \leq \epsilon_0$ the following is true:

$$\text{(i)} \quad \| h[\theta, z(\theta, y_0, \theta_0)] - x[\theta, h(\theta_0, y_0), \theta_0] \| \leq \delta, \qquad \theta \in [\theta_0, \theta_0 + L/\epsilon] \quad \text{(A11)}$$

Here $z(\theta, y_0\theta_0)$ is the solution of the initial value problem for Eq. A10 with $z(\theta_0) = y_0$ such that the resulting $z(\theta)$, $\theta \in (\theta_0, \infty)$, belongs to Ω together with its σ-vinicity; $x(\theta, x_0, \theta_0)$ is the solution of the initial value problem for Eq. A4 with $x(\theta_0) = x_0 = h(\theta_0, y_0)$.

(ii) Whenever Eq. A10 has the equilibrium point that is globally asymptotically stable, inequality Eq. A11 holds for all $\theta \in (\theta_0, \infty)$.

(iii) Whenever Eq. A10 has a locally asymptotically stable equilibrium point z_s, Eq. A8 has an asymptotically stable period solution $y^*(\theta)$, $\theta \in (-\infty, \infty)$, and $\|\bar{x}_s(y^*) - \bar{x}_s(z_s)\| < \delta$. Here $\bar{x}_s(y^*)$ is the average steady state of Eq. A4

$$\bar{x}_s(y^*) = \lim_{T\to\infty} \frac{1}{T} \int_0^T h[\theta, y^*(\theta)]\, d\theta, \qquad \text{(A12)}$$

and $\bar{x}_s(z_s)$ is the approximated average steady state of Eq. A4

$$\bar{x}_s(z_s) = \lim_{T\to\infty} \frac{1}{T} \int_0^T h(\theta, z_s)\, d\theta. \qquad \text{(A13)}$$

Propositions 1 and 2 constitute the method of analysis of dynamic systems with fast deterministic parametric oscillations. The proof of these propositions can be found in Bellman et al. (1983b).

Literature cited

Aris, R., and N. R. Amundson, "An Analysis of Chemical Reactor Stability and Control," *Chem. Eng. Sci.*, **7**(3), 121 (1958a); 132 (1958b); 148 (1958c).

Ausikaitis, J., and A. J. Engel, "Steady State Multiplicity and Stability in an Adiabatic Controlled, Cycled, Stirred-Tank Reactor," *AIChE J.*, **20**, 256 (1974).

Bailey, J. E., "Periodic Operation of Chemical Reactors: A Review," *Chem. Eng. Commun.*, **1**, 111 (1973).

———, "Periodic Phenomena," *Chemical Reactor Theory*, L. Lapidus and N. R. Amundson, eds., Wiley, New York (1977).

Bailey, J. E., and F. J. M. Horn, "Comparisons between Two Sufficient Conditions for Improvement of an Optimal Steady State Process by Periodic Optimization," *J. Optim. Theory Appl.*, **5**, 378 (1971).

Bellman, R., J. Bentsman, and S. M. Meerkov, "Vibrational Control of Systems with Arrhenius Dynamics," *J. Math. Anal. Appl.*, **91**, 152 (1983a).

———, "Nonlinear Systems with Fast Parametric Oscillations," *J. Math. Anal. Appl.*, **97**, 572 (1983b).

———, "Vibrational Stabilizability of Nonlinear Systems," *Proc. 9th World IFAC Cong.*, **8**, 53, Budapest (1984a).

———, "Vibrational Control of Nonlinear Systems," *Proc. 23rd Control Decision Conf.*, **1**, 84, Las Vegas (1984b).

Bogoliubov, N. N., and Yu. A. Mitropolsky, *Asymptotic Methods in the Theory of Nonlinear Oscillations*, Gordon and Breach, New York (1961).

Bruns, D. D., and J. E. Bailey, "Process Operation Near an Unstable Steady State Using Nonlinear Feedback Control," *Chem. Eng. Sci.*, **30**, 755 (1975).

———, "Nonlinear Feedback Control for Operating a Nonisothermal CSTR Near an Unstable Steady State," *Chem. Eng. Sci.*, **32**, 257 (1977).

Chang, M., and R. A. Schmitz, "An Experimental Study of Oscillatory States in a Stirred Reactor," *Chem. Eng. Sci.*, **30**, 21 (1975a).

———, "Feedback Control of Unstable States in a Laboratory Reactor," *Chem. Eng. Sci.*, **30**, 837 (1975b).

Cinar, A., J. Deng, S. M. Meerkov, and X. Shu, "Vibrational Control of an Exothermic Reaction in a CSTR: Theory, Simulation, Experiment," *AIChE Ann. Meet.*, San Francisco, Paper No. 101b (1984).

Ding, J. S. Y., S. Sharma, and D. Luss, "Steady State Multiplicity and Control of the Chlorination of Liquid *n*-decane in an Adiabatic CSTR," *Ind. Eng. Chem. Fundam.*, **13**(1), 76 (1974).

Douglas, J. M., *Process Dynamics and Control*, Prentice-Hall, Englewood Cliffs, NJ (1972).

Fjeld, M., "Asynchronous Quenching of Nonlinear Systems Exhibiting Limit Cycles," *IEEE Trans. Auto. Control*, **AC-13**, 201 (1968).

———, "Relaxed Controls in Asynchronous Quenching and Dynamical Optimization," *Chem. Eng. Sci.*, **29**, 921 (1974).

Gilbert, E. G., "Optimal Periodic Control: A General Theory of Necessary Conditions," *J. Optim. Theory Appl.*, **15**, 717 (1977).

Lin, K. F., "Multiplicity and Uniqueness for Binary, Exothermic Reaction in a Nonadiabatic Continuous Stirred-Tank Reactor," *Chem. Eng. Sci.*, **35**, 1537 (1980).

Matsubara, M., Y. Nishimura, and N. Takahashi, "Optimal Periodic Control of Lumped-Parameter Systems," *J. Opt. Theory Appl.*, **13**, 31 (1974).

Meerkov, S. M., "Principle of Vibrational Control: Theory and Applications," *IEEE Trans. Auto. Control*, **AC-25**(4), 755 (1980).

———, "Condition of Vibrational Stabilizability for a Class of Nonlinear Systems," *IEEE Trans. Auto. Control*, **AC-27**(2), 485 (1982).

Minorsky, N., *Nonlinear Oscillations*, Van Nostrand, Princeton, NJ (1962).

Rinaldi, S., "High-Frequency Optimal Periodic Processes," *IEEE Trans. Auto. Control*, **AC-15**, 671 (1970).

Root, R. B., and R. A. Schmitz, "An Experimental Study of Steady State Multiplicity in a Loop Reactor," *AIChE J.*, **15**(5), 670 (1969).

Schmitz, R. A., R. R. Bautz, W. H. Ray, and A. Uppal, "The Dynamic Behavior of a CSTR: Some Comparisons of Theory and Experiments," *AIChE J.*, **25**(2), 289 (1979).

Uppal, A., W. H. Ray, and A. B. Poore, "On the Dynamic Behavior of Continuous Stirred-Tank Reactors," *Chem. Eng. Sci.*, **29**, 967 (1974).

———, "The Classification of the Dynamic Behavior of Continuous Stirred-Tank Reactors—Influence of Reactor Residence Time," *Chem. Eng. Sci.*, **31**, 205 (1976).

Vejtasa, S. A., and R. A. Schmitz, "An Experimental Study of Steady State Multiplicity and Stability in an Adiabatic Stirred Reactor," *AIChE J.*, **16**, 410 (1970).

Manuscript received Aug. 15, 1985, and revision received July 8, 1986.